Novel Adsorbent from Biowaste (Shrimp Shells): Metal-Impregnated Activated Carbon for Efficient Dye

N Annlin Bezy [1*], K Francy [2†], A Lesly Fathima [3‡]

[1] *Register No 20213042132006, Research Scholar, Research Department of Physics, Holy Cross College, Nagercoil*

[2] *Department of Chemistry, Holy Cross College, Nagercoil – 4*

[3] *Research Department of Physics, Holy Cross College, Nagercoil – 4 (Affiliated to Manonmanium Sundararnar University, Tirunelveli)*

Abstract

Activated carbon (AC) is a valuable material utilized in multiple sectors owing to its ver- satility and ability to absorb various compounds effectively. Its adsorption characteristics are due to a large surface area and extensive porous network. Metal impregnation into acti- vated carbon is for the improvement of its adsorption capacity and the elimination of specific contaminants like heavy metals, organic pollutants, or gases assessing with long-term per- formance. The chitosan derived from shrimp shells has the property of dye adsorption. Such a polymer chitosan with adsorption property is reformed into activated carbon by pyrolysis to enhance its adsorption ability in the removal of hazardous dyes. Field Emission Scanning Electron Microscopy (FESEM) of the AC showed a porous surface. Aluminium (Al), Iron (Fe), and Silver (Ag) were incorporated into the activated carbon individually by simple chemical method, at low temperatures. The structural investigation results give the Ag-imposed AC forms in a polycrystalline phase with crystallite size in the nanoscale. FTIR data of metal- imposed AC proves that chemical modification occurs in activated carbon by the inclusion of metals. The adsorption of Rhodamine 6G and Amaranth dyes by AC/Al, AC/Fe, and AC/Ag were investigated by UV analysis. This work shows that about 47% concentration of Amaranth dye was adsorbed by AC/Al composite, and to the maximum 21% of Rhodamine was adsorbed by AC/Ag sample in an experiment time of 10 hours at room temperature.

Keywords: Activated Carbon; Dye Adsorption; Porosity; Metal; Shrimp shells

*E-mail: leslysat@gmail.com

†E-mail: francyscc28@gmail.com

‡E-mail: leslysat@gmail.com

1 Introduction

Adsorption is a process that has a strong ability to extract impurities. The materials with great absorbance performance hold a wide range of applications. Because, it is a basic, easy-to-scale technique that effectively traces the contaminants. Adsorbents derived from the food processing wastes, production wastes, recycling products will result low cost, resourceful compound. The biomass-drawn adsorbent material requires stability, better efficiency, and modifiable to increase the versatility. Biomass contains rich quantity of compounds including proteins, lipids, minerals, cellulose, hemicellulose, lignin's, phenol compounds and acetyl groups etc. The pretreatment of biomass acts the major role in defining the characteristics of yielded adsorbent, in the factors like adsorption adequacy, size of particles, purity of the material. The pretreatment eliminates unnecessary compounds and contaminating agents.

Adsorption is an ancient man-made technique, implemented by using activated charcoal in vast fields, with long-lasting performance. This single technique holds application in various ranges from air to water purification. Some examples are chemical and dye industries the effluent water treatment, household drinking water purification systems, beverage manufacturing the activated carbon-based compound is highly utilized. The activated carbon may effectively remove anionic and cationic dyes, reactive and hazardous chemicals, organic solutes. The mostly used form of activated carbon in eliminating contaminants are layer filtration, electrochemical treatment, oxidation. The maximum adsorbent can get from the agriculture and marine food processing industries on daily basis. Due to the plenty of availability, the biomass derived adsorbent is considered my many research sectors. The metal-activated carbon matrix also acts as an adsorbent in reducing harmful dyes like Rhodamine 6G, Amaranthus, Methyl orange etc, at room temperature. The inclusion of metal to the activated carbon modifies its porosity, hence surface area facilitates to degrade the dyes. The major problem as of from the industries are manufacturing waste during the fabrication/ production from a wide range of industrial activity. Water is a necessary compound to form a healthy ecosystem and sustainable human life. The industrial dye waste can contaminate the water resulting harmful to aquatic plants, and animals entirely indulging the ecotoxicological system.

Aquaculture generated food is rich with nutrition and taking major role in economy of small- and large-scale industries in many countries. While the processing of sea food, enormous wastes was generated and the direct discharge may lead to cause contamination of microorganisms. Being the untreated wastes fill the land, the shrimp shell has multipurpose usages, rich with nutrients which can be utilized as feed for animals, resource for agriculture and the source of bioactive compounds (polymer) [1]. The production of activated carbon is a way that shrimp waste might be considered. The structure of organic carbon produced from biochar's will have different chemical properties.

Researchers are drawn to the activated carbon, carbon-based structure found in biochar because it can be used as a filter membrane, an adsorbent, and a capacitive material with high efficiency. There are numerous researchers working to produce nano 2D and 3D structures using carbon extracted from shrimp shells. The purity, stability, non- toxic, biocompatibility and crystallinity are the necessary factors which has been concentrated in production of carbon and carbon composites [2]

2 Materials and Methods

2.1 Chemicals Used

The Aluminium Nitrate, Silver Nitrate and Ferrous Nitrate salts were purchased in AR grade with high purity from Loba chemicals. The Rhodamine 6G and Amaranth dyes were purchased from Sigma Aldrich.

2.2 Experimental Details

The shrimp shells collected from the food processing industry was initially washed and treated in 1N of HCl for the removal of mineral content and followed by the diluted NaOH to eliminate the proteins in raw shells. Finally, the obtained chitin was treated by 10N of NaOH in 75C for 2 hours. After neutralizing, the chitosan obtained is dried in hot air oven at 100C. The extracted chitosan is subjected to slow pyrolysis under 450C for two hours. The obtained product is activated carbon.

An easy chemical procedure was used to synthesize the AC/metal (Ag, Fe and Al) composites. 250 mg of activated carbon (AC) was taken in the beaker. For one hour, 2M of ferrous nitrate, silver nitrate and aluminium nitrate salts were taken in separate beakers, dissolved in double distilled water (DDW) to produce a clear solution. In the magnetic stirrer, activated carbon (AC) was added to this solution and mixed for two hours at room temperature. The mixture was then ultrasonicated for 60 minutes, and then it was washed with ethanol and deionized water. The corresponding AC/Fe, AC/Ag, and AC/Al composite samples that sedimented in the bottom of beaker was then collected for analysis and dried at 100°C in a hot air oven.

2.3 Preparation of Dyes

The organic dyes Rhodamine 6G and Amaranth were purchased for dye adsorption studies. Initially, the stock solution of Rhodamine 6G was prepared in volumetric flask by taking 95.8 mg/L in double distilled water. The prepared concentrated solution was diluted in double distilled water (DDW) in the ratio 3:1 respectively. In magnetic stirrer, the mixture was mixed for few hours and diluted dye was collected for adsorption analysis.

For the preparation of Amaranth stock solution, 60.4 mg/L of Amaranth was taken in double distilled water (DDW). The prepared stock solution of Amaranth dye diluted in DDW in the 3:1 ratio respectively. The diluted dye was mixed using magnetic stirrer until complete amalgamation and the finally collected for adsorption analysis.

2.4 Adsorption Experiment

To the prepared dyes of Rhodamine 6G and Amaranth in the ratio of 3:1, the 0.5 g/L of prepared metal imposed activated carbon composites (AC/Fe, AC/Al, and AC/Ag) were taken respectively. Subsequently, the dye with samples were kept in the magnetic stirrer at room temperature for the adsorption to takes place. For every two hours the degraded dye was collected for analysis. The UV analysis was taken to evaluate the adsorption by the AC/metal composites.

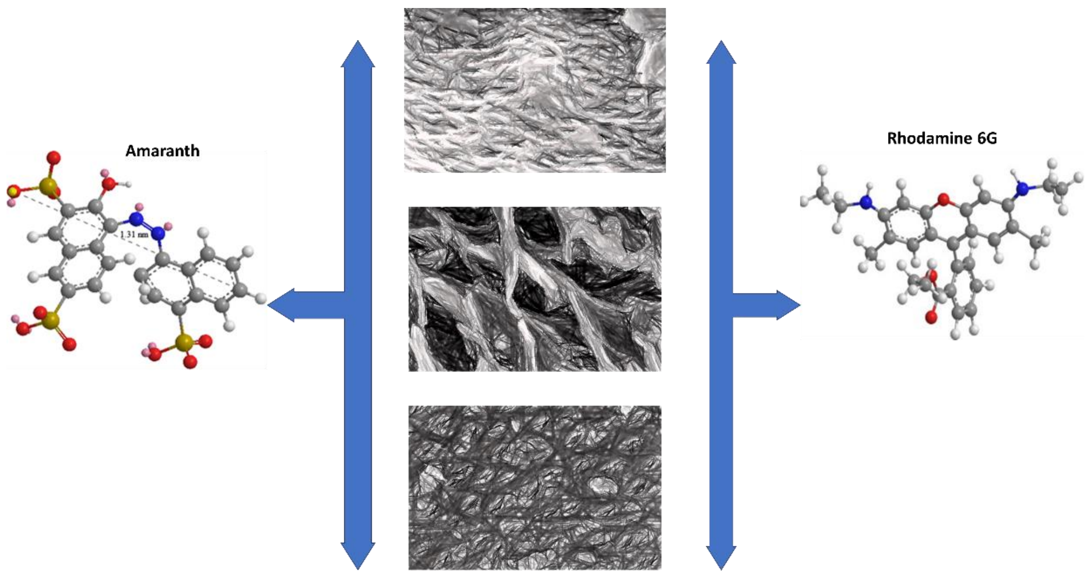

Figure 1 Pictorial diagram representing structure of dyes and morphology of produced composites

Techniques Implemented

The shrimp shell derived activated carbon-based AC/Fe, AC/Al, and AC/Ag composites phase were analyzed from the X-Ray diffraction using the Bruker D8 Advance instrument in the radiation of CuKα 1.5418Å wavelength with the voltage of 40kV and current 30 mA. The morphology of composites was observed from FESEM taken in SIGMA HV – Carl Zeiss with Bruker Quantax 200 – Z10 EDS Detector from CIT, Coimbatore. The adsorption of dye by the produced material was studied from UV analysis which was done using UV-1800 Series in the wavelength range of 200 nm to 800 nm, in absorbance mode.

Result And Discussion

X-Ray Diffraction

The XRD pattern of AC/Fe, AC/Al, and AC/Ag were given in Fig. 2. The graph of AC/Al reveals a broad peak of amorphous carbon at 24.44° angle, validates the AC/Al composite material's amorphous phase. A non-existent metal peak is the result of low temperatures involved in the present synthesis. The other reason behind is presence of minimum percentage of aluminium in the AC/Al composites [3]. Sharp iron peaks are absent in the XRD pattern of an AC/Fe composite, indicating a good dispersion of ferrous nitrate on activated carbon. There are not any significant differences in the amorphous phase of the graph, particularly has a hump at angles 25°, 43°, and 65° [4], [5], [6]. Hence, concludes the activated carbon-iron composites is in amorphous phase. In the graph of AC/Ag, the characteristics peaks of both activated carbon and silver are existing which found as wide, sharp peaks. Ag/AC shows a large peak at angle 25.22°, which corresponds to the 002 planes of AC, and sharp peaks at angle (2θ) of 38.08°, 44.18°, 64.23°, and 77.27°, which correspond to the hkl planes of (111), (200), (220), and (311) to silver, respectively. The polycrystalline nature of the composite is demonstrated through its purity, crystallinity, and grain size [7], [8], [9]. Being as polycrystalline form, the crystallite size was calculated using Scherrer's equation $D = k \lambda / \beta \cos \theta$, and the average crystallite size was found to be as 35.98nm.

https://doi.org/10.46947/joaasr6420248

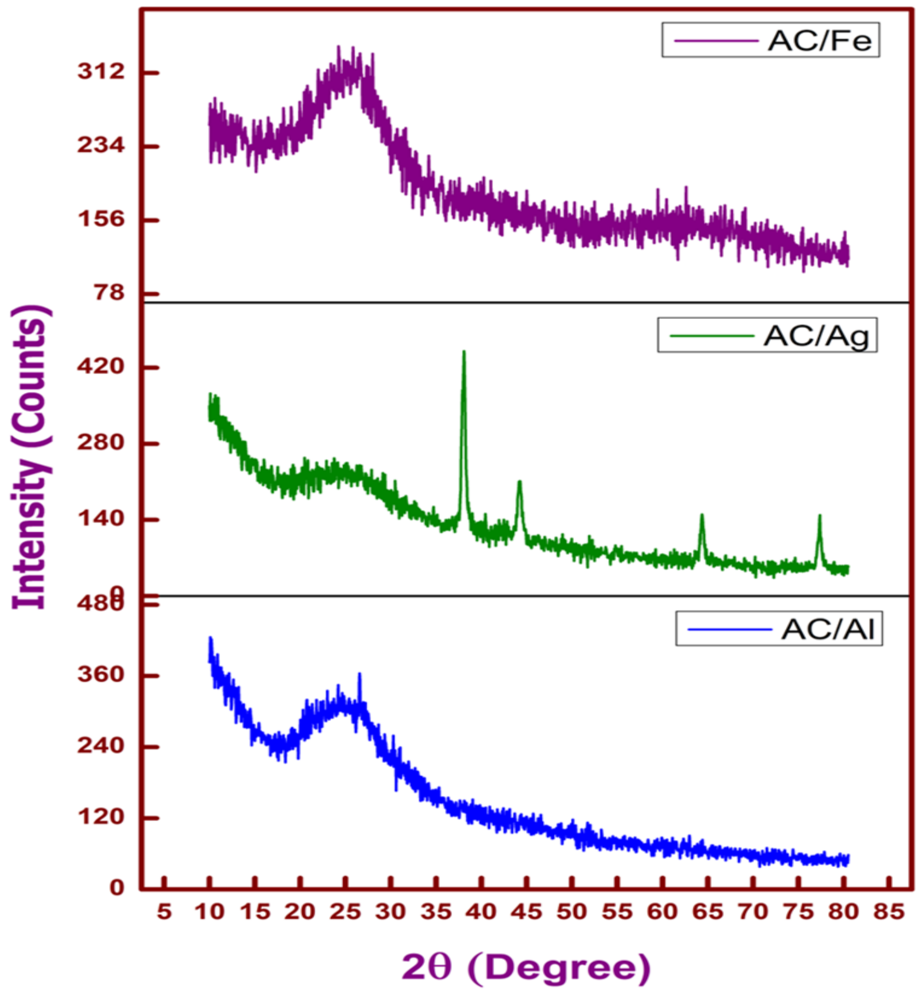

Figure 2 XRD pattern of synthesized AC/metal composites

Field Emission Scanning Electron Microscopy

The morphology of synthesized composites can be seen in Fig. 3. The Fig. 3 (a) shows the morphology of shrimp shell derived activated carbon, resembles the porosity with rupturing walls. Though the surface looks similar in entire image, and the hole sizes are in micro range. The FESEM image of AC/Fe in Fig. 3 (b) shows significant change from the AC morphology. When iron is incorporated on carbon, cavities are formed across the surface of the carbon. The cavities shape looks as ellipse with pointed edges and the number of porous is minimized than the AC. The image shows the porosity of the carbon, with sides appears as a smooth surface. The given image of low magnification also shows tiny particles scattered throughout the surface. However, the porosity forms seem to be similar. The morphology of AC/Ag is given in Fig. 3 (c). In silver incorporated AC composite the porosity appears like scaffold form. However, the depiction of the scaffold's nanoscale range indicates that its walls are thin. Further, the low magnification images resemble grains scattered across the surface and this suggests that the hole in AC may contain the element silver.

https://doi.org/10.46947/joaasr6420248

FESEM image in Fig. 3 (d) is the AC/Al composites morphology, shows porosity with modifications compared to activated carbon (AC) FESEM images. The porous formed looks like deep holes with wall thickness in nanoscale. The given micro-range image of the AC/Al also revealed some rough surface or humb at the edge of the holes. Thus, note the obvious change caused by the presence of Al in this region [10].

The presence of homogenous porosity in all synthesised composites is demonstrated by the FESEM information. The surface roughness is also observed throughout, this specifies the high surface area. The adsorption of pollutants, colours, and gases may be favoured by the porous material, which is evident from the Fig. 3, however those will be examined from adsorption analysis in this work [11]. This report investigates the (Rhodamine 6G and Amaranth) dye adsorption by produced AC/Al, AC/Fe, and AC/Ag composites.

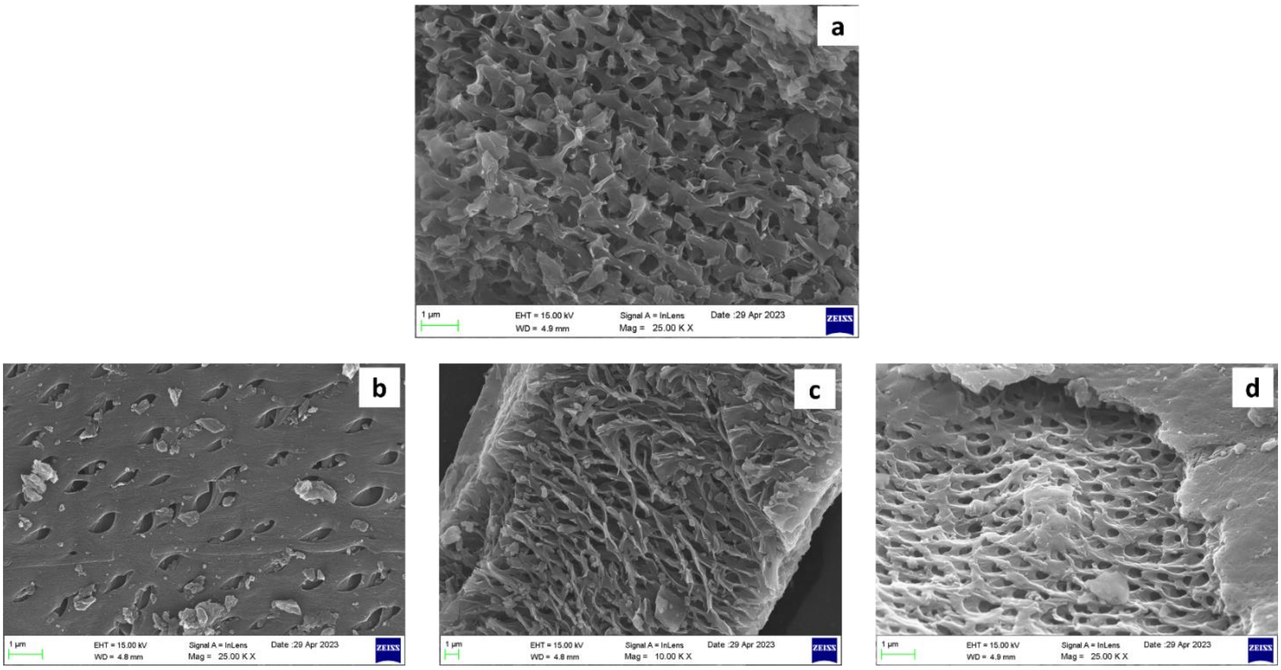

Figure 3 FESEM of (a) Activated Carbon (b) AC/Fe (c) AC/Ag and (d) AC/Al

Energy-Dispersive X-Ray Spectroscopy

According to the EDS results, the metals (Al, Ag, and Fe) have been successfully incorporated into the activated carbon. The EDX spectra of produced AC/Al, AC/Fe and AC/Ag composites is given in Fig. 4. The carbon content with a noticeable peak displays a high percentage in all three spectrums. Since carbon is the main component in the generated matrix, it is seen in the largest amount. With an atomic percentage of 3.92, the composite formed by Ag has a higher incorporation percentage among the three taken elements Al, Fe, and Ag. Being, in EDX the Ag holds valuable percentage, it can also be previously explored in XRD with the characteristics silver peaks. On the other hand, the EDS validates the creation of novel- material with distinct qualities appropriate for adsorption. The percentage of elements in the produced composites were listed in Table.1

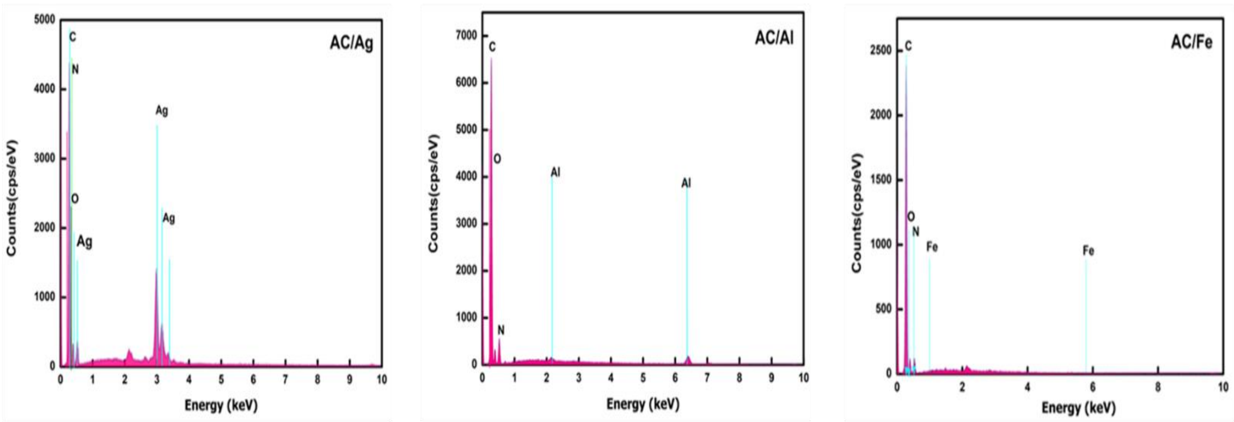

Figure 4 EDX spectrum of synthesized AC/metal composites

Table 1 EDX data of synthesized composites

	Element	**Weight (%)**	**Atomic (%)**
AC/Fe	Carbon Nitrogen Oxygen Iron	62.87 24.07 13.01 0.12	67.39 22.13 10.43 0.05
AC/Al	Carbon Nitrogen Oxygen Aluminium	59.17 20.62 17.26 2.94	65.42 19.55 14.33 0.70
AC/Ag	Carbon Nitrogen Oxygen Silver	43.44 18.26 13.49 24.81	60.10 21.76 14.08 3.86

Fourier Transform Infrared Spectroscopy

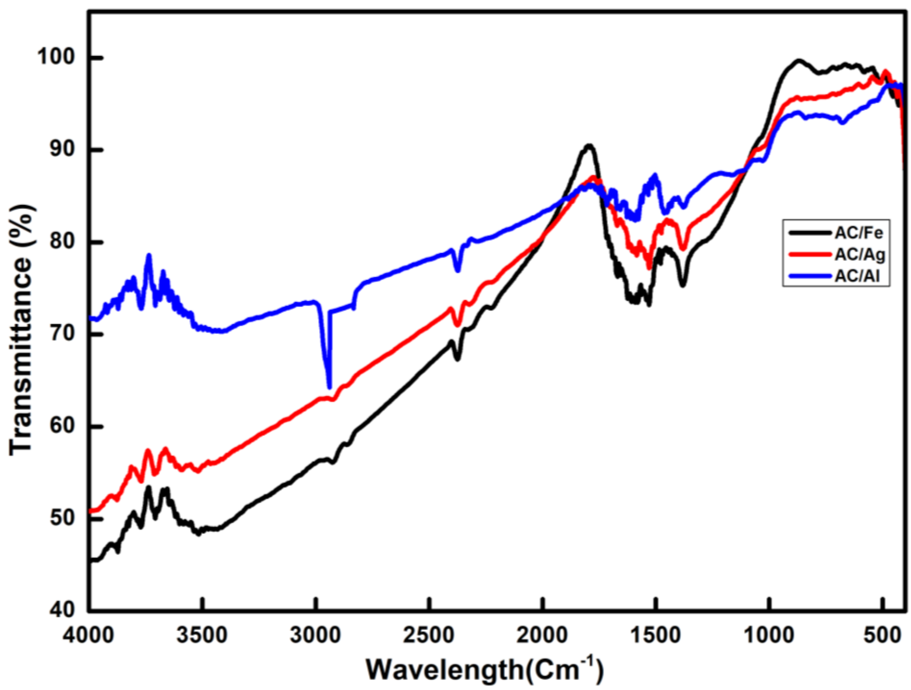

Figure 5 FTIR spectra of AC/metal composites

Fourier transform infrared spectroscopy spectra of AC/metal (Fe, Ag, Al) is presented in Fig. 5. The band formed at 3591 – 3512 cm^{-1} in three spectra were attributed to O-H stretching. The strong peak at 2929 cm^{-1} due to C-H bending is formed in the AC/Fe composite. In the other two spectrums this band can be seen with lower transmittance. At 2374 cm^{-1} the band corresponding to C-O stretching is found, confirming the existence of carboxylic acid. However, the functional groups within the prepared activated carbon composites impacts its adsorption ability, catalysts and ion exchanges [12]. The surface modification from the activated carbon in carbon, oxygen and hydrogen bonds of the synthesized composites evidences the existence of metal.

Adsorption Studies

Using UV-Vis's spectroscopy, the maximum wavelengths of Rhodamine 6G and Amaranth dye were 542 nm and 533 nm, respectively. This wavelength is considered to measure the dye concentration in the supernatant.

The dye removal percentage R (%) was corresponding to time t, was calculated using the formula R (%) = $[(C_0-C_t)/C_0]$ *100, where C_0 (mg. L^{-1}) and Ct (mg. L^{-1}) are the concentration at initial and certain time t (min).

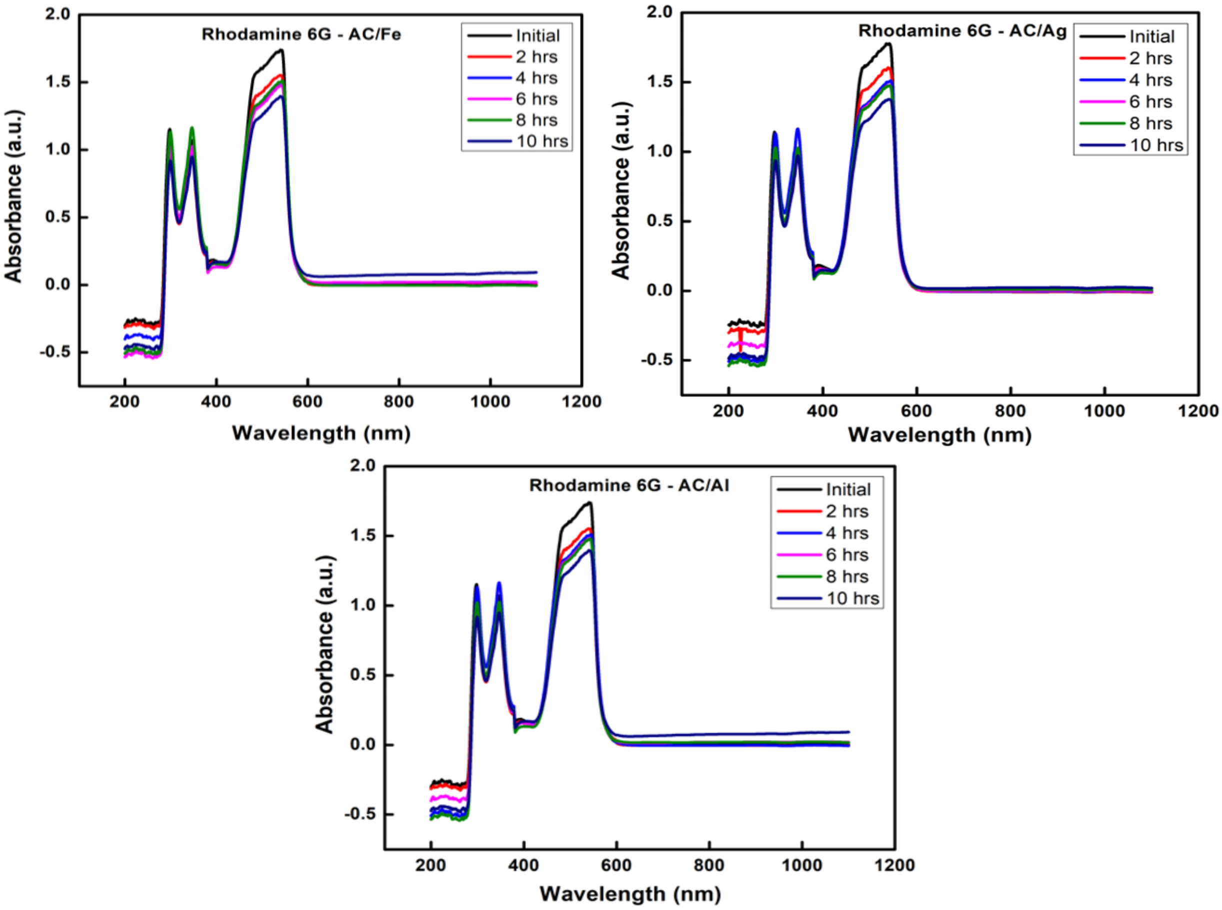

Figure 6 UV absorbance spectra of Rhodamine 6G dye by AC/metal composites

The adsorption of Rhodamine 6G by AC/Al, AC/Fe, and AC/Ag composites is rapid during the initial duration for 2 hours. The high chemical potential of the synthesised metal composites allows for the quick adsorption of dye. The adsorption remains delayed in the further contact time of composites with the dye. However, the all-synthesized particles show distinguished degradation for every 2 hours of period. Among the three metals (Fe, Al, Ag) the silver imposed activated carbon has greater dye removal efficiency with 20.99% of concentration of dye after 10 hours of experiment time. The UV spectra gives the primary absorbance as 1.7 (a.u.) and after the experiment time it decreases to 1.3 (a.u.), 1.4 (a.u.), and 1.39 (a.u.) for AC/Ag, AC/Al and AC/Fe respectively which is illustrated in Fig. 6. Hence proven, the synthesized metal imposed activated carbon will ensure as an adsorbent for the removal of toxic dyes from pigment productions [13], [14].

Table 2 Adsorption data of Rhodamine 6G

Dye	**AC/metal composite**	**Efficiency of dye (%)**					**Maximum Absorption (nm)**
		2 hrs	4 hrs	6 hrs	8 hrs	10 hrs	
Rhodamine 6G	AC/Fe	11.4	14.86	14.86	13.13	20	542
	AC/Al	10.93	13.58	14.96	15.19	19.67	
	AC/Ag	7.83	13.75	15.01	15.24	20.99	

The adsorption spectra of composites AC/Al, AC/Fe, and AC/Ag observed in amaranth dye is given

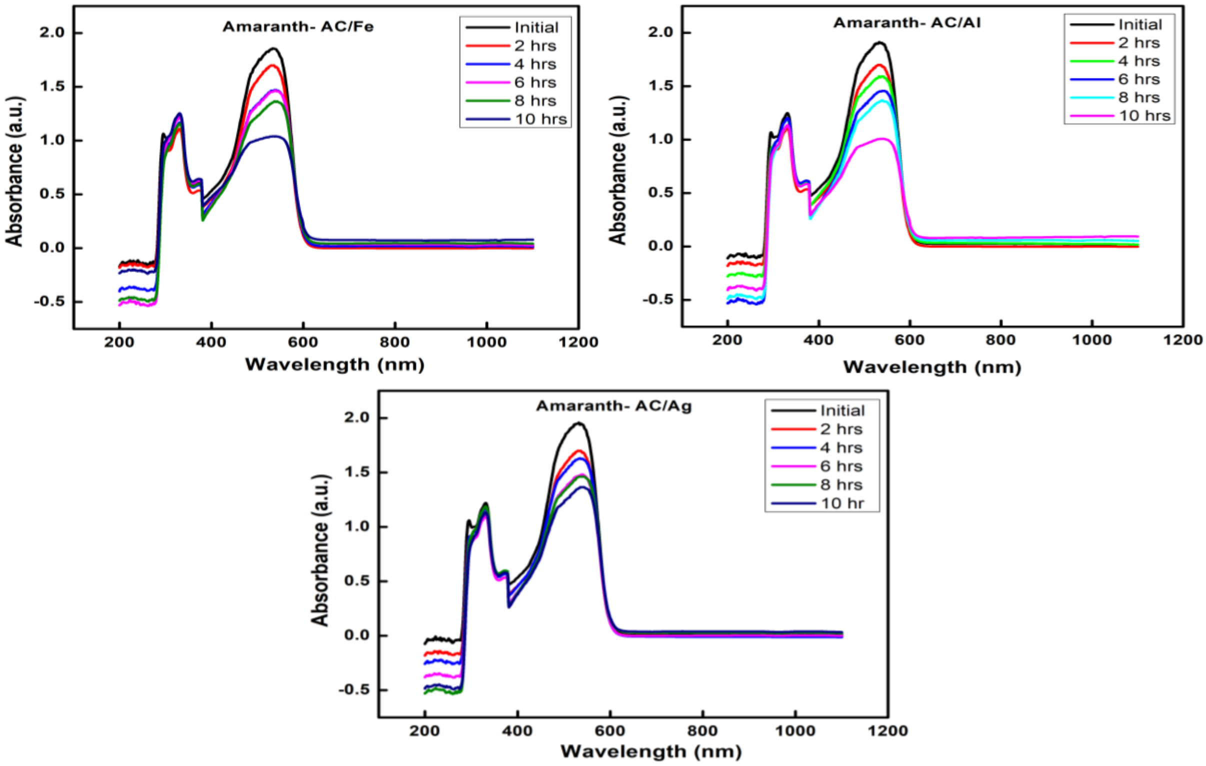

Figure 7 UV absorbance spectra of Amaranth dye by AC/metal composites

in Fig. 7. The absorbance value of UV spectra decreases from 1.9 (a.u.) to 1 (a.u.), 0.9 (a.u.), 1.3 (a.u.) in AC/Fe, AC/Al, and AC/Ag respectively. During the entire durations of experimental time the adsorption rate is moderate. The equilibrium state was established in 6 hours of adsorbing time, where the sample reaches maximum efficiency. In amaranth dye investigation Al incorporated AC performs maximum adsorption with 46.91%.

Table 3 Absorption data of Amaranth

Dye	AC/metal composite	Efficiency of dye (%)					Maximum Absorption (nm)
		2 hrs	4 hrs	6 hrs	8 hrs	10 hrs	
Amaranth	AC/Fe	8.47	21.14	21.57	26.42	44.05	533
	AC/Al	10.64	16.78	24.01	28.52	46.91	
	AC/Ag	13.06	16.84	24.47	25.03	30.46	

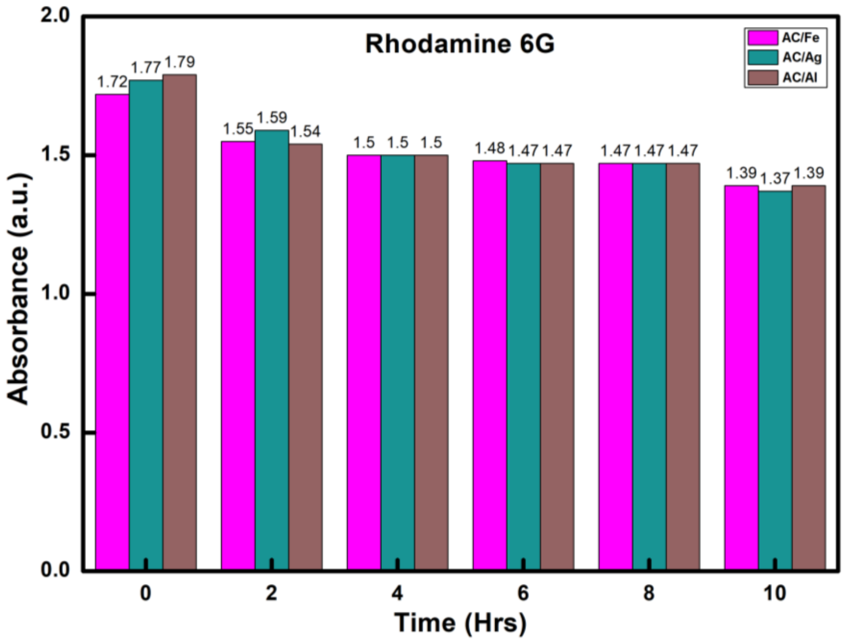

Figure 85 Rhodamine 6G absorbance Bar diagram

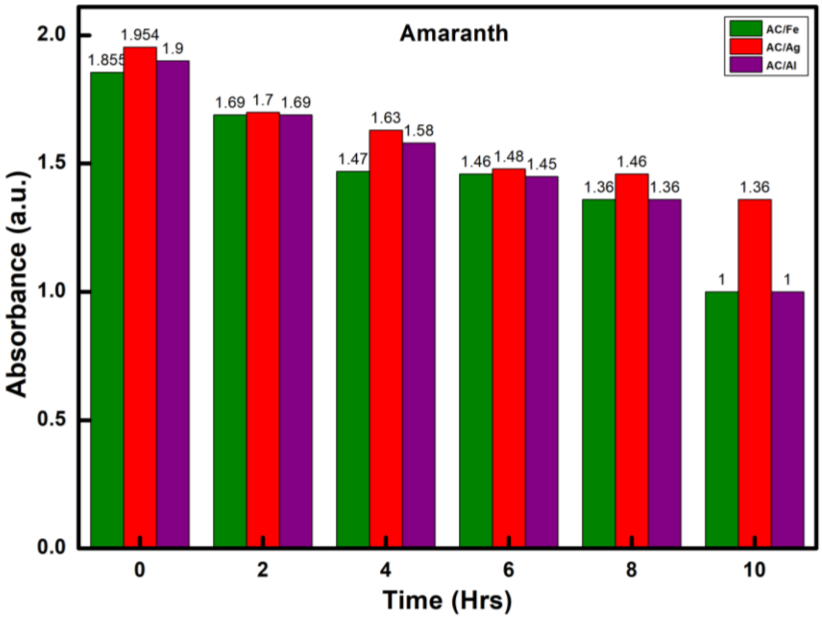

Figure 6 Amaranth absorbance bar diagram

The Fig. 8 and 9 describes the absorbance value of dye in relation to time using the bar diagram. In decision, the amaranth is highly removed comparing to the rhodamine dye. The significant role of metal incorporated (Fe, Al, Ag) activated carbon as a adsorbent material performs better. The distinct feature of the composite is fabrication of porosity and high surface in material without any peripheral means. The adsorption of amaranth and rhodamine 6G were occurs through the electrostatic interaction, carbon, hydrogen bonding between the molecular ions in dye and existing functional groups in the AC/ metal (Fe, Ag, Al) composites, in addition its influence by surface area and porous. The tables 2 and 3 gives the adsorption rate of rhodamine 6G and amaranth in the corresponding hours. Under normal circumstances, the maximum percentage of amaranth and rhodamine 6G degradation is 46% and 20%, respectively, without the use of a catalyst such as irradiation or temperatures.

CONCLUSION

The marine crustacean (Shrimp Shells) derived activated carbon was successfully produced. Metals (Al, Ag, Fe) were incorporated into the activated carbon by chemical method, using harmless corresponding nitrate salts. The phase of the produced composites was analysed and among, the silver incorporated activated carbon forms in polycrystalline nature. The morphology of composites reveals the formation of modified surface by the incorporation of metals to AC. EDX proves the presence of imposed metals with activated carbon, being minimum percentage the morphology is greatly influenced by the metals. This emphasizes the importance of using it to remove contaminants (dye) and purify pollutants. The adsorbing efficiency of the metal composites that were produced is higher in Amaranth dye than in Rhodamine 6G dye, according to the absorption research of the composites conducted in Rhodamine 6G and Amaranth UV analysis results. However, by increasing the quantity of adsorbent relative to the dye the 100% efficiency must be attained in minimum time.

Graphical Representation

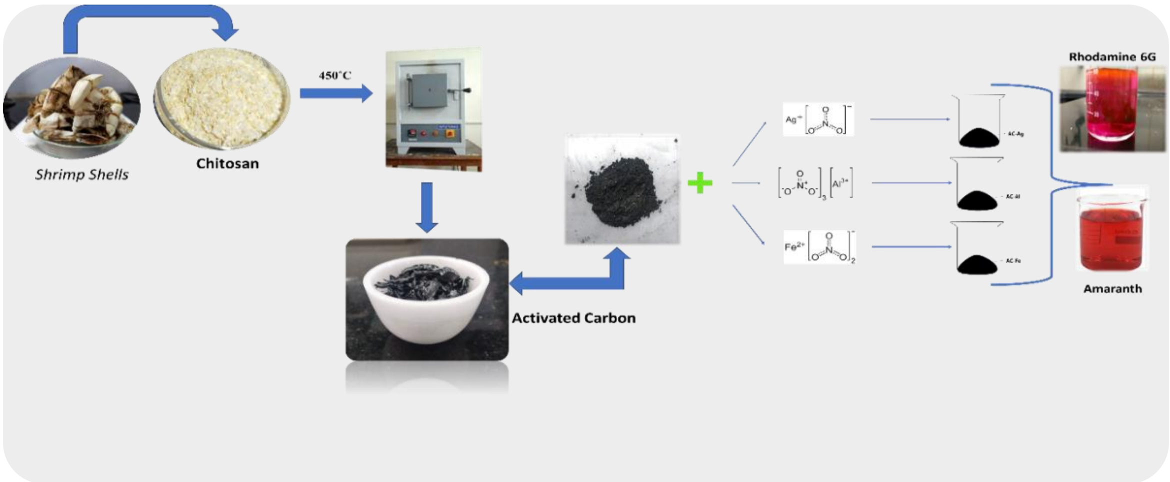

Highlights

- Metal impregnated activated carbon prepared by chemical method
- Unique porous were formed in the prepared composites
- Harmful dyes amaranth and rhodamine 6G can be removed successfully
- Minimum percentage of metal can improve its adsorption efficiency

References

[1] O. A. Salawu, Z. Han, and A. S. Adeleye, "Shrimp waste-derived porous carbon adsorbent: Performance, mechanism, and application of machine learning," J. Hazard. Mater., vol. 437, p. 129266, Sep. 2022, doi: 10.1016/j.jhazmat.2022.129266.

[2] A. S. Adeleye, K. T. Ho, M. Zhang, Y. Li, and R. M. Burgess, "Fate and Transformation of Graphene Oxide in Estuarine and Marine Waters," Environ. Sci. Technol., vol. 53, no. 10, pp. 5858–5867, May 2019, doi: 10.1021/acs.est.8b06485.

[3] S. Bakhta et al., "Functional activated carbon: from synthesis to groundwater fluoride removal," RSC Adv., vol. 12, no. 4, pp. 2332–2348, 2022, doi: 10.1039/D1RA08209D.

[4] X. Zhang, Y. Li, G. Li, and C. Hu, "Preparation of Fe/activated carbon directly from rice husk pyrolytic carbon and its application in catalytic hydroxylation of phenol," RSC Adv., vol. 5, no. 7, pp. 4984–4992, 2015, doi: 10.1039/C4RA13248C.

[5] Z. Gu, J. Fang, and B. Deng, "Preparation and Evaluation of GAC-Based Iron-Containing Adsorbents for Arsenic Removal," Environ. Sci. Technol., vol. 39, no. 10, pp. 3833–3843, May 2005, doi: 10.1021/es048179r.

[6] F. M. Duarte, F. J. Maldonado-Hódar, and L. M. Madeira, "Influence of the iron precursor in the preparation of heterogeneous Fe/activated carbon Fenton-like catalysts," Appl. Catal. A Gen., vol. 458, pp. 39–47, May 2013, doi: 10.1016/j.apcata.2013.03.030.

[7] H. Chandra Joshi, D. Dutta, N. Gaur, G. S. Singh, R. Dubey, and S. K. Dwivedi, "Silver-doped active carbon spheres and their application for microbial decontamination of water," Heliyon, vol. 8, no. 4, p. e09209, Apr. 2022, doi: 10.1016/j.heliyon.2022.e09209.

[8] R. Al-Gaashani, D. Almasri, B. Shomar, and V. Kochkodan, "Preparation and properties of novel activated carbon doped with aluminum oxide and silver for water treatment," J. Alloys Compd., vol. 858, p. 158372, Mar. 2021, doi: 10.1016/j.jallcom.2020.158372.

[9] C. Karthik and K. V Radha, "Silver Nanoparticle Loaded Activated Carbon: An Escalated Nanocomposite with Antimicrobial Property," Orient. J. Chem., vol. 32, no. 1, pp. 735–741, Mar. 2016, doi: 10.13005/ojc/320182.

[10] L. de Oliveira Pereira, I. Marques Sales, L. Pereira Zampiere, S. Silveira Vieira, I. do Rosário Guimarães, and F. Magalhães, "Preparation of magnetic photocatalysts from TiO2, activated carbon and iron nitrate for environmental remediation," J. Photochem. Photobiol. A Chem., vol. 382, p. 111907, Sep. 2019, doi: 10.1016/j.jphotochem.2019.111907.

[11] G. Horvat, M. Pantić, Ž. Knez, and Z. Novak, "A Brief Evaluation of Pore Structure Determination for Bioaerogels," Gels, vol. 8, no. 7, p. 438, Jul. 2022, doi: 10.3390/gels8070438.

[12] J. Gao et al., "Adsorption of methylene blue onto activated carbon produced from tea (Camellia sinensis L.) seed shells: kinetics, equilibrium, and thermodynamics studies," J. Zhejiang Univ. Sci. B, vol. 14, no. 7, pp. 650–658, Jul. 2013, doi: 10.1631/jzus.B12a0225.

[13] S. Phoemphoonthanyakit, P. Seeharaj, P. Damrongsak, and K. Locharoenrat, "Effect of Adsorption Characteristics of Rhodamine 6G Dye Solution in Fe 3 O 4 Magnetic Nanoparticles on Fluorescence Quantum Yield," J. Spectrosc., vol. 2019, pp. 1–5, Jul. 2019, doi: 10.1155/2019/2853989.

[14] N. Van Hung et al., "Highly effective adsorption of organic dyes from aqueous solutions on longan seed-derived activated carbon," Environ. Eng. Res., vol. 28, no. 3, pp. 220116–0, May 2022, doi: 10.4491/eer.2022.116.